[20] M. P. Ekstron, W. D. McCaa, Jr., and N. S. Nahman, "The measured time and frequency response of a miniature superconducting coaxial line," *IEEE Trans. Nuclear Sci.*, vol. NS-18, pp. 18–25, Oct. 1971.
[21] K. Mikoshiba, a letter to the author reporting the status of Hitachi Research Laboratory's work, Jan. 27, 1971.
[22] ——, a letter to the author reporting the status of Hitachi Research Laboratory's work, June 14, 1971.
[23] ——, a letter to the author reporting the status of Hitachi Research Laboratory's work, Oct. 25, 1971.
[24] Y. Hoshiko, Electrical Communication Laboratory, Nippon Telegraph and Telephone Public Corp., Tokyo, Japan, a letter to the author describing technical details of the improved lines studied at NTT, Dec. 20, 1971.
[25] Y. Hoshiko and N. Chiba, "Superconductive communication cables" (in Japanese), *Oyo Buturi*, vol. 40, pp. 905(83)–906(84), Aug. 1971.
[26] ——, "Superconductive cable communication system" (in Japanese), *J. Inst. Elec. Commun. Eng. Japan*, vol. 55, pp. 184–189, Feb. 1972.
[27] K. Mikoshiba, N. Omori, F. Sone, and N. Chiba, "Discussion of superconductive coaxial cables" (in Japanese), in *Proc. 1972 Nat. Conf. Inst. Elec. Commun. Eng. Japan* (Tokyo, Japan, Apr. 3–6, 1972), p. 1460.
[28] N. Chiba, Y. Hoshiko, and H. Yahagi, "Characteristics of superconductive coaxial cables" (in Japanese), in *Proc. 1972 Nat. Conf. Inst. Elec. Commun. Eng. Japan* (Tokyo, Japan, Apr. 3–6, 1972), p. 1459.
[29] Y. Kashiwayanagi, J. Shirokawa, and N. Chiba, "Design of superconductive coaxial cables" (in Japanese), in *Proc. 1972 Nat. Conf. Inst. Elec. Commun. Eng. Japan* (Tokyo, Japan, Apr. 3–6, 1972), p. 1461.
[30] Y. Kashiwayanagi, J. Shirokawa, S. Sentsui, and N. Chiba, "Superconductive coaxial cable," Central Research Laboratory, Furukawa Electric Co., Ltd., Tokyo, Japan, Tech. Rep. TI-71039, Apr. 1972.
[31] Y. Kashiwayanagi, S. Sentsui, J. Shirokawa, and N. Chiba, "Tan δ and ϵ_r of dielectrics at 4.2°K, 1 GHz," Central Research Laboratory, Furukawa Electric Co., Ltd., Tokyo, Japan, Tech. Rep. TI-71040, Apr. 1972.
[32] S. Ramo, J. R. Whinnery, and T. Van Duzer, *Fields and Waves in Communication Electronics*. New York: Wiley, 1965, p. 333 and p. 444.
[33] H. Hahn, H. J. Halma, and E. H. Foster, "Measurement of the surface resistance of superconducting lead at 2.868 GHz," *J. Appl. Phys.*, vol. 39, pp. 2606–2609, May 1968.

Weakly Superconducting Circuits

HARRIS A. NOTARYS, RUN-HAN WANG, AND JAMES E. MERCEREAU

***Abstract*—An equivalent circuit has been developed for the time-dependent dissipating state of superconductivity which accompanies quantum phase slip. This equivalent circuit is used here to analyze the superconducting thin-film ring magnetometer and to determine its operating characteristics in terms of measurable circuit parameters.**

INTRODUCTION

ELECTRONIC applications of superconductivity generally involve the behavior of a superconductor at finite voltage. These applications fall into two general classes: one centers on circuits utilizing the very low resistance of a superconductor, and the second involves more explicit macroscopic quantum phenomena. This paper will discuss some thin film devices from this second class in terms of their equivalent circuits.

The heart of all of the superconducting quantum devices is Josephson's original prediction [1] relating supercurrent through barriers to quantum phase. For the superconducting tunnel junction this relationship can be written in terms of supercurrent density j_s and voltage V as:

$$j_s = j_0 \sin \frac{2e}{\hbar}\left(\int V dt + \alpha\right)$$

where $h/2e$, the quantum of flux, is often denoted by ϕ_0 and α is a phase angle determined by magnetic flux. This unusual relationship arises from the macroscopic quantum nature of superconductivity and predicts that a constant voltage applied to a Josephson tunnel junction produces an oscillating supercurrent of amplitude j_0 at frequency $\omega = 2eV/\hbar$. However, in the usual electronic application these junctions are not driven at constant voltage but are included in more general circuits. It has been found that a useful equivalent circuit for the superconducting tunnel junction element can be obtained by augmenting the Josephson current by parallel resistive and capacitive current paths. Many models [2] of this type have been invented which seem to describe the behavior of Josephson tunnel junctions at finite voltage with reasonable success.

A second type of superconducting junction involves more complex contortions of the superconducting state. In the tunnel junction, the basic time dependence involves only the relative quantum phase $\Delta\phi$ across the junction. It is the evolution of this phase difference, $\Delta\phi = \phi_0^{-1}(\int V dt + \alpha)$ which controls the supercurrent. There is another class of Josephson device, the genesis of which is the Dayem [3] bridge, in which both the amplitude and phase of the macroscopic quantum state are time dependent. This time-dependent quantum process is called "phase slip" [3]; the *amplitude* of the quantum state goes instantaneously to zero within a small region of the superconductor and recovers while the relative phase across this region changes by 2π. In this situation dissipation by the superconducting state itself becomes an important concept and the equivalent circuit for this process cannot fully be described by the addition of parallel components to a Josephson tunnel junction. We will discuss an equivalent circuit for

Manuscript received June 2, 1972; revised August 28, 1972. This work was partially supported by the Office of Naval Research under Contract N00014-67-A-0094-0013.

The authors are with the California Institute of Technology, Pasadena, Calif. 91109.

dissipating junctions of this type in the following section and emphasize the dissipation aspects by adapting a description in terms of potential rather than supercurrent.

Dissipation Potential in Weak Superconductors

In this section we describe how voltage is developed by the process of phase slip dissipation. This is somewhat equivalent to describing quantum transitions of this macroscopic quantum state. Phase slip is a local process in the superconductor during which superconductivity is destroyed in a small region extending roughly over the coherence distance ξ. During phase slip the amplitude of the macroscopic quantum state goes to zero and recovers—the time scale for this is of the order of $\tau \sim h/\Delta \sim 10^{-11} - 10^{-12}$ s, and the relative quantum phase across the region of decay changes by 2π. The energy loss per electron in this instantaneous destruction of superconductivity is the superconducting energy gap potential Δ and for the entire circuit amounts to $\bar{I}_s\phi_0$, where $\bar{I}_s$ is the average of the supercurrent existing before and after slip.

It has been shown [4] that above the critical current in sufficiently small superconducting structures a repetitive phase slip process occurs at a repetition rate given by $\omega = 2e/\hbar V$. In an attempt to characterize this dynamic superconducting process we have developed structures ("junctions") in which we can control the phase slip and have measured many aspects of this process. We believe that phase slip in these junctions is a nonpropagating process in which the superconducting amplitude and phase are time dependent but there is no motion involving the transport of quantized flux. Contrary to the tunnel junction, these structures operate by a basically discontinuous irreversible process which consumes power. Power consumed by this type of junction will be the normal V^2/R plus a non-ohmic superconducting dissipation equal to the loss per slip ($\bar{I}_s\phi_0$) multiplied by the number of slips per second $V\phi_0^{-1}$ or $\bar{I}_sV$.

Measurement [5] and analysis [4] of the potential developed by dissipation across these small phase slip structures shows that for currents I greater than the critical current I_c the potential V resulting from discontinuous phase slip can be approximated by the following continuous function in most circumstances:

$$V = RI - \tfrac{1}{2}RI_c(B, T)\left\{1 + \cos\frac{2e}{\hbar}\int (Vdt + \alpha)\right\} \quad (1)$$

where R is the resistance of the junction in the normal state, I_c is a function of both magnetic field B and temperature T, and α accounts for any current at zero voltage. In small junctions at low voltage the magnetic field dependence of I_c is similar to that of a Josephson tunnel junction [5]. This approximation (1) is of course not entirely accurate in a physical sense especially near the gap frequency, since it approximates a discontinuous process. Nevertheless, it has proved to be a generally useful function with which to describe dissipation in our superconducting circuits. The dissipation voltage V (or the energy loss per electron in traversing the junction) is less than in the normal state (IR) by a time-dependent quantity which we call the Josephson potential. For a sufficiently short junction the magnitude of this potential ($\frac{1}{2}RI_c$) depends only on the energy gap of the superconductor Δ and as for the Josephson tunnel junction, is approximately [6] Δ/e. To emphasize the non-ohmic nature of this dissipation we define $v_s = \frac{1}{2}RI_c$ and write an "Ohm's Law" for these weak superconductors as

$$V = IR - v_s(T, B)\left\{1 + \cos\frac{2e}{\hbar}\left(\int Vdt + \alpha\right)\right\}. \quad (2)$$

This potential is both time and temperature dependent. At temperatures and currents where $v_s \ll IR$ the voltage V developed from a given current I is nearly constant with time average $\bar{V} = IR - v_s$ and with only a small time varying component $V_s(t) = v_s \cos(2e/\hbar)\bar{V}t$. However, when $v_s \sim \frac{1}{2}RI$, the amplitude of V is strongly time dependent even for constant I leading to extreme anharmonic voltages—becoming pulselike with an amplitude $\sim RI$, width $\tau = \phi_0(RI)^{-1}$, and repetition rate $\nu = \bar{V}\phi_0^{-1}$. Equations (1) and (2) appear to have general validity for these specially prepared phase slip junctions in most situations using measured values for R and I_c. These expressions have been experimentally tested by measurements on the amplitude, frequency, and frequency spectrum of the time-dependent voltage developed from a current source. In addition, current–voltage curves have been measured in a wide variety of circumstances with both current and voltage sources at various frequencies.

By inspection of (2) it is evident that the equivalent circuit for these phase slip circuits is a resistor (R) in *series* with a voltage source $v_s\{1 + \cos(2e/\hbar)\int(Vdt + \alpha)\}$. In using this equivalent circuit it must be kept in mind that v_s is not a source of power. The circuit only expresses the fact that the weak superconductor dissipates less than the normal state at a given current—the energy loss per electron V is less than IR. On the other hand, it also indicates that a weak superconductor dissipates *more* than the normal state at a given voltage.

With this equivalent circuit for the phase-slip process we can do circuit analysis of more complex superconducting circuits containing this type of junction. The general procedure will be to use (2), and the equivalent circuit for phase slip, to account for dissipation in these superconducting circuits. In this way the dynamics of the circuit can be completely described as the response of the circuit to a power source. By directly specifying the dissipation in the circuit in terms of the quantum periodicity, as we do in (2), the dynamic properties of the circuit are a necessary result, even in a nonequilibrium dissipating state.

Simple Circuits

In this section we use (2) to describe the behavior of a phase slip junction in a superconducting ring, fundamentally a junction shorted by a superconducting inductor. This particular circuit forms the basis for many of the present superconducting magnetometers. Most of the early analysis [7], [8] of superconducting magnetometer circuits was based on the equilibrium characteristics of the magnetic flux enclosed by these circuits. This equilibrium flux varies periodically with the applied flux, with period ϕ_0. While this type of analysis and its extensions [9] certainly give the general features of the magnetometer circuit we can now determine the dynamics of the flux change in terms of the circuit parameters and dissipation in the circuit and design these and other circuits for optimum performance. Our basic approach will be to use (2) in conjunction with Kirchhoff's laws to analyze this simple circuit.

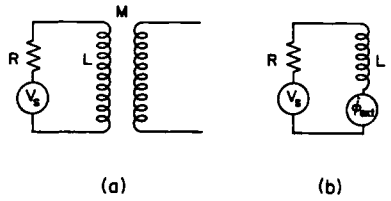

Fig. 1. Schematic representation of the magnetometer ring circuit (resistance R and inductance L) inductively coupled (M) to a power source. In (b) the power source is approximated as a voltage source ($\dot{\phi}_{ext}$) in the magnetometer ring circuit.

Physically, the junction acts as the dissipation which allows flux to change in the ring circuit. This dissipation is the energy lost to phonons via phase slip, $I_s\phi_0$. And this energy is exactly equal to the difference in energy between two adjacent quantized flux states of the inductor

$$\frac{1}{2L}n^2\phi_0^2 - \frac{1}{2L}(n-1)^2\phi_0^2.$$

However, it is the potential V which determines the dynamics of the dissipation and thus the rate of the quantum response of the circuit. In order to make use of (2) to describe the ring circuit, we assume that the superconducting ring is also coupled inductively to a power source in such a way that this source can be approximated by a voltage source in the ring circuit $\dot{\phi}_e$, see Fig. 1.

This assumption explicitly implies that flux is not necessarily quantized in this description of the superconducting ring but only that the rate of change of the relative quantum phase across the junction is set by the voltage V. The phase angle α in this circuit is determined by the magnetic flux Φ through the ring at the instant that the voltage is zero—which occurs twice per cycle for a harmonic voltage source. Thus applying Kirchhoff's law to the circuit, including (2), gives

$$V = \dot{\phi}_e - L\dot{I} = RI - v_s \cdot \left\{1 + \cos\frac{2e}{\hbar}\left(\int V dt + \Phi\right)\right\} \quad (3)$$

and the solution to (3) will give the complete analytic form for the current in the ring circuit as a function of drive voltage $\dot{\phi}_e$. However, since (3) only applies for current in excess of the critical current I_c, a simple harmonic drive flux can lead to serious complications in the analysis. The current then will also be quasi-harmonic, passing through zero twice per cycle, and for a time be less than critical. A complete analyses of (3) must take this into account. Such an analysis is beyond the scope of this paper and here we will assume that I_c is sufficiently small relative to the total current that a continuous solution of (3) to a harmonic drive flux is a valid approximation.

Equation (3) is basically nonlinear and considerable caution must be exercised in any approximation so as not to approximate away real effects. Our approach will be to assess the variation from classical behavior which results from the potential v_s. From that point of view, we can conceptually separate the response into two parts: a classical response of induced current in a ring, and a variation in this classical response due to quantum effects characterized by v_s. The variation in current caused by the quantum effects can then be written as

$$\delta I_s \approx \frac{v_s}{R + i\omega L}\left\{\cos\frac{2e}{\hbar}\left(\int V dt + \Phi\right)\right\} \quad (4)$$

where V must be determined from the total circuit response to drive flux. When $R \gg \omega L$, inspection of (4) shows that the effect of v_s is largely dissipation reflecting an energy loss per electron of $R\delta I$, but for $R \ll \omega L$, v_s shows up as an EMF destroying an amount of flux $L\delta I$. Thus in the limit $R \gg \omega L$ the quantum effects will show up predominantly as dissipation (or an effective parametric resistance) while when $R \ll \omega L$ the main effect will be a modification of flux (or thus an effective parametric reactance). As we indicate in (3), V is applied voltage $\dot{\phi}_e$ minus the EMF of the inductor $L\dot{I}$. If quantum effects are small then the current can be approximated classically in terms of the voltage $\dot{\phi}_e$ and impedance $Z = R + i\omega L$ as, $I \simeq \dot{\phi}_e/Z$ and $V \simeq (R/Z)\dot{\phi}_e$.

In this limit then

$$\delta I_s = \frac{v_s}{Z}\left\{\cos\left[\frac{2e}{\hbar}\left(\frac{R}{Z}\right)\phi_e(t)\right]\cos\frac{2e}{\hbar}\Phi - \sin\left[\frac{2e}{\hbar}\left(\frac{R}{Z}\right)\phi_e\right]\sin\frac{2e}{\hbar}\Phi\right\}. \quad (5)$$

If $\phi_e(t) = \phi_e \sin \omega t$ then (5) can be expanded in harmonics to show that the magnitude of δI at the drive frequency is

$$\delta I_s = \left(\frac{v_s}{Z}\right)J_1\left\{\frac{R}{Z}\phi_e'(t)\right\}\sin\Phi' \quad (6)$$

where ϕ_e' and Φ' are, respectively, the RF and dc flux in units of $\hbar/2e$. Thus in this particular limit quantum effects modify the current by an amount represented by (6). This modification of current also shows up in the driving circuit as a reflected "quantum voltage" $V_{RF} = i\omega M\delta I$

$$|V_{RF}| = v_s\left(\frac{\omega M}{Z}\right)J_1\left(\frac{R}{Z}\phi_e'\right)\sin\Phi'. \quad (7)$$

If $R \gg \omega L$ expression (7) can be written in terms of an equivalent resistance δR by equating (7) to a resistive potential $I\delta R$ and

$$\delta R = \frac{v_s}{I}\left(\frac{\omega M}{R}\right)J_1(\phi_e')\sin\Phi' \quad (8a)$$

or if $R \ll \omega L$ as an equivalent reactive impedance

$$\omega\delta L = \frac{v_s}{I}\left(\frac{M}{L}\right)J_1\left(\frac{R}{\omega L}\phi_e'\right)\sin\Phi'. \quad (8b)$$

Thus the effect of the superconducting ring circuit can be represented as an effective resistance δR or reactive impedance $\omega\delta L$. These parameters will modify the characteristics of the circuit to which the ring is coupled. If this is a resonant tank circuit, as is usually the case, then the main effect of δR will be a change in Q while the main effect of $\omega\delta L$ will be a shift in resonance frequency. For this reason we have referred to the effects of $R > \omega L$ ring circuits as amplitude modulation (AM) and $R < \omega L$ circuits as frequency modulation (FM). These induced changes in the impedance of the tank circuit depend parametrically on both the RF and dc magnetic flux

and are used as the basis for magnetometer circuits as we discuss in the next section.

Expression (6) will be valid as long as the voltage V is predominantly determined by the classical impedance. This will be true while v_s is sufficiently small. But since v_s is a function of temperature, increasing with decreasing temperature, at low temperature the approximations which lead to (6) may no longer be valid. This will begin to occur when V is significantly perturbed by quantum effects. Since $V=\dot{\phi}-L\dot{I}$ we can estimate the variation of V due to the quantum modification of current δI_s as $\omega L\delta I_s$. This variation in V leads to a variation in the instantaneous frequency of $\delta\Omega\sim\omega L\delta I_s\phi_0^{-1}$. In order to keep these self-modulation effects small, $\delta\Omega/\omega$ must be small. Therefore, the requirement that (6) be valid is $L\delta I_s\phi_0^{-1}<1$ or

$$v_s < \phi_0\left|\frac{Z}{L}\right| = \omega\phi_0\left|1+i\frac{R}{\omega L}\right|$$

or

$$I_c < \omega\phi_0\left|\frac{1}{R}+\frac{i}{\omega L}\right|. \tag{9}$$

If $R>\omega L$ then the limit is $I_c<\phi_0/L$ while when $R<\omega L$, the limit on I_c is

$$I_c < \frac{\omega\phi_0}{R} \quad (\text{or } RI_c < \omega\phi_0).$$

Thus for high-resistance circuits ($R>\omega L$) the region of validity of (6) is the usually recognized limit $I_c<\phi_0/L$ while for low-resistance circuits the criteria is $RI_c<\omega\phi_0$, which for these junctions is independent of the cross sectional area of the junction. For this reason we find that it is often not useful to make particularly narrow phase slip junctions and have used junctions up to 1 mm wide.

When v_s exceeds the value set by (9), the circuit is no longer able to follow the influence of the drive voltage in the simple manner expressed by (6). The harmonic response then gives way to a pulse-like response. As v_s increases above (9), the voltage V which determines the *frequency* at which the circuit responds becomes dominated by the dynamics of the circuit itself and there are strong feedback effects. As previously indicated, this feedback results in an internal frequency of $\Omega\sim(\omega L/Z)(v_s/\phi_0)$. Thus as v_s greatly exceeds the limits set by (9) this internal frequency becomes very large. And since at very high frequency inductive impedance will dominate the circuit the internal frequency approaches v_s/ϕ_0. This is the rate at which the circuit will react above the limit set by (9). The result is a "voltage pulse" of amplitude v_s whose time duration is $\phi_0 v_s^{-1}$. This "voltage pulse" is in reality the spontaneous dissipation incurred during phase slip and represents a loss of electromagnetic energy into phonons. However, even in this limit this dissipation will show up in the circuit either resistively or inductively depending on the circuit parameters. The effect of the external drive $\phi_{ext}(\omega)$ is simply to trigger these pulses and supply the energy that is dissipated by the pulse voltage. This limit has been analyzed previously [8] and it was found that this situation produces a signal with large harmonic content whose amplitude at the drive frequency (ω) is

$$\delta I_s \sim \frac{\dot{\phi}_e}{Z}\, J_1\left(\frac{R}{Z}\,\phi_e'\right)\sin\Phi'. \tag{10}$$

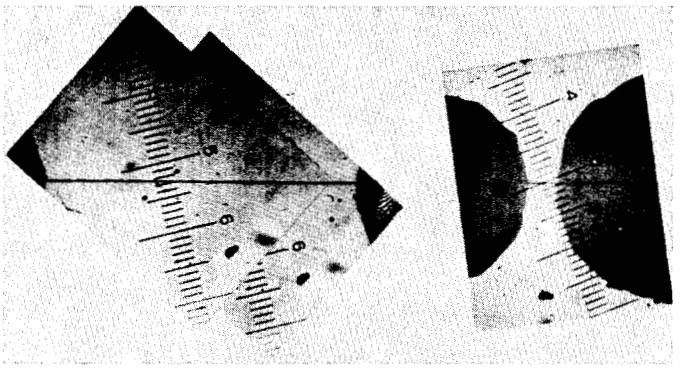

Fig. 2. Microphotograph of a phase slip junction in a hard superconductor. Scale is about 6.5 μ/div.

As v_s increases, the drive flux ϕ_e also becomes modified by shielding effects. As a first approximation to this effect we reduce the drive flux by a flux equivalent to the shielding current I_c (defined as ϕ_c) or $\dot{\phi}\simeq(\phi_e-\phi_c)\omega$. With this additional approximation (10) becomes:

$$\delta I_s \sim \frac{\omega(\phi_e-\phi_c)}{Z}\, J_1\left(\frac{R}{Z}\,(\phi_e'-\phi_c')\right)\sin\Phi'. \tag{11}$$

Thus as v_s increases the quantum response will go from a form proportional to the first-order Bessel function in ϕ_e to a form with a "critical flux." Above the critical flux the current generally increases with increasing ϕ_e in a periodic manner until it reaches a maximum of about $\omega\phi_0/Z$ and then gradually decreases.

Experimental Results

Thin-film structures with controllable parameters were developed in order to investigate this phase slip process. Basically, a small region of known dimensions in a superconducting thin film was made more weakly superconducting than the film proper. This region, which has a depressed transition temperature, acted to confine the location of phase slip. This was achieved in two ways. For soft superconductors such as Sn, In, Pb, a narrow thin-film line of normal material such as Au or Cu was first fabricated on a glass substrate using plastic scratching or photo-etching techniques. Then this line was overlayed with a superconductor to form an alloy or layered region of depressed transition temperature. For hard supperconductors such as Nb, Ta, W, and Re the superconducting film, on a sapphire substrate, was thinned by anodization along a line bisecting the film; consequently depressing the transition temperature in this region (see Fig. 2).

It was possible to controllably vary the characteristic parameters of these structures including the transition temperature, normal resistance, critical current, material, and dimensions—thickness, width, and length along current direction. General features of the phase slip process were determined by investigation of these parameters over the following ranges—length <0.5 to $10^3\mu$, width 1 to $10^3\mu$, thickness 50 to 3000 Å, normal resistance 10^{-3} to 10 Ω, transition temperature 1.3 to 9K. The general features were independent of material. The only critical dimensional dependence was on the length which should be less than a micron for best results. Much longer junctions become noisy because of the lack of definition of the phase slip region along the current path. The junction operation depended strongly on the product of normal resistance and critical current RI_c, but there was no direct dependence on width. Finally, RI_c also determined the noise char-

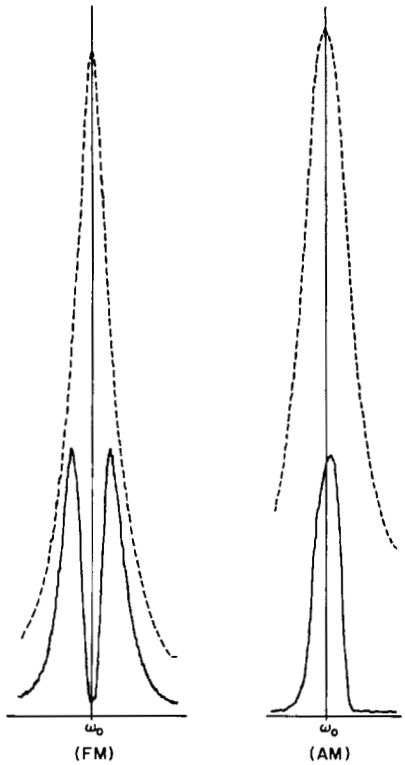

Fig. 3. Dashed line is the impedance of the magnetometer circuit as a function of frequency. Solid curve is the amplitude of the variation of this impedance upon changing the magnetic field by one quantum. Data on left are for $R<\omega L$, on right for $R\sim\omega L$.

acteristics of the junction. Consequently, as a result of these investigations and using measured R and I_c, it is possible to describe the electrical characteristics of limited length junctions ($\sim 1\ \mu$) by (2).

In this section we briefly review a few experimental results obtained with these circuits. A typical circuit is a thin-film cylindrical ring, diameter and length each 3 mm, evaporated on a sapphire rod. The ring also contains a phase slip junction. This ring is inductively coupled to a tank circuit resonant at about 30 MHz and thus modifies the effective impedance of this circuit. Variations in the effective impedance due to superconducting quantum effects such as represented in (8a), (8b), and (11) are reported here. Characteristic circuit parameters were: For the tank circuit $L_T \simeq 10^{-7}$ H, $C_T \simeq 300$ pF with $Q \simeq 450$, and the coupling of the rod to the tank was $M^2/L_r L_T \simeq 0.03$. The ring inductance L_r was $\simeq 2\times 10^{-9}$ H, and the junction parameters were varied widely: Length 0.5 to 30 μ, width 1 to 300 μ, thickness 100 to 1000 Å, transition temperatures 2 to 5K, normal resistance 10 mΩ to 1 Ω for both hard and soft superconductors.

Fig. 2 shows a microphotograph of a phase slip junction in a hard superconducting thin-film ring. This same junction was tested at two different widths to examine the effects of resistance relative to inductive impedance as expressed in (8). In the photograph on the left of Fig. 2 the junction is 1.1 μ long and 282 μ wide and has a resistance about 1/10 the inductive impedance. On the right of Fig. 2 the junction has been narrowed to 20 μ and the inductive and resistive impedances are approximately equal.

Fig. 3 shows the variation in impedance caused by the two circuits represented in Fig. 2. All of these data were taken at temperatures where $v_s < \omega\phi_0[1+i(R/\omega L)]$. On the left, labeled FM, is the impedance variation caused by the superconducting ring circuit containing the wide junction, $R<\omega L$. The dashed curve is the magnitude of the impedance of the tank circuit (with inductively coupled superconducting ring) as a function of frequency near the resonance frequency. The solid curve is the maximum excursion in this impedance caused by a one quanta change in the constant magnetic field through the ring. The magnitude of this excursion is symmetric about the resonance frequency and is of opposite sign on opposite sides of the resonance. These results are indicative of a frequency modulation effect and are what were anticipated from (8b) in terms of an effective parametric inductive impedance for the ring circuit in this limit.

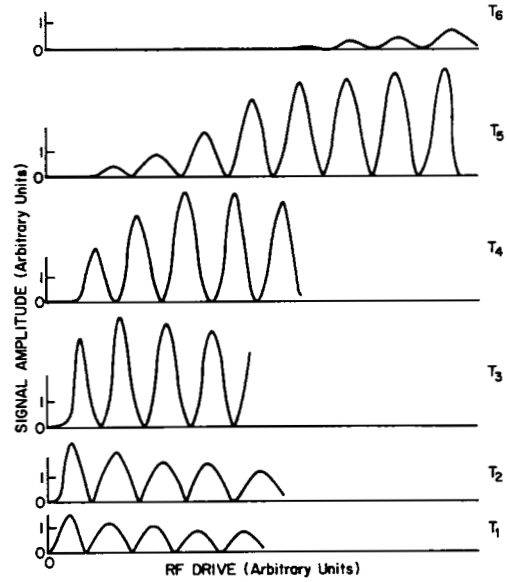

Fig. 4. Temperature dependence of the magnetometer response as a function of RF drive. Data taken at ω_0 for (AM) case of Fig. 3.

To the right in Fig. 3 are the results for the same circuit when $R\sim\omega L$. In this case the variation in the impedance is nearly symmetric and always of the same sign. This response is indicative primarily of AM and again is what was anticipated in (8a) when the principal effect of the superconducting ring is as a parametric resistance. The RF drive levels required for maximum response in these two situations also differed by approximately the ratio of 10:1, ($\omega L/R$(wide):1), as expected from (8). By driving the tank circuit from a constant current source this variation in impedance shows up as a signal voltage which is often used as the basis for magnetometer circuits. More detailed analysis of the circuit shows that this signal is largest for $R<\omega L$ circuits where for optimum coupling it becomes $\omega\phi_0$.

The amplitude of the signal voltage as a function of temperature is shown in Fig. 4 in a situation when $R\sim\omega L$. This signal amplitude represents an excursion in impedance resulting from a change in the constant field Φ by one quantum. This excursion is periodic in Φ, with period ϕ_0, however, the signal amplitude is also a periodic function of drive level as shown in Fig. 4. Actually, the amplitude changes sign with alternative periods as would be expected from the Bessel character of (8) and (10) but the data are plotted in amplitude only. At the highest temperature T_1, where $v_s \ll \omega\phi_0[(1+i(R/\omega L))]$ the first-order Bessel response to RF drive is clearly evident. As the temperature decreases to T_2 this amplitude increases. At T_3 we see the first clear onset of a critical current (or critical flux) effect and at lower temperatures the pure Bessel character changes to a more

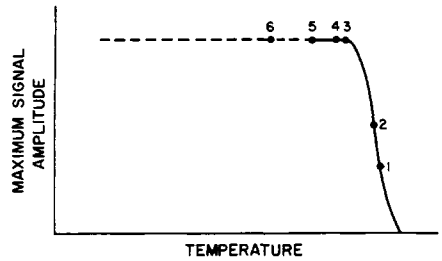

Fig. 5. Maximum magnetometer signal amplitude as a function of temperature.

complex amplitude response—first increasing then decreasing with increasing drive as anticipated in (11). As the temperature decreases below T_6 the same general response continues but requires higher and higher drive levels. The quantum signal seems to persist to the lowest temperatures but at a drive level set by the critical current.

Maximum signal amplitude as a function of temperature is shown in Fig. 5. For these data, the signal was maximized at each temperature as a function of RF drive and this maximum was recorded as a function of temperature. Near the transition temperature, the signal increases rapidly with decreasing temperature as does v_s until it saturates at about $\omega\phi_0$ and then remains constant with decreasing temperature.

Summary

We have found that the operation of simple superconducting phase slip circuits can be characterized in terms of their electrical circuit parameters and critical current. These results are characteristic of all the devices of this type which we have tested regardless of material. By varying the relative dimensions (and therefore circuit parameters) we are able to obtain either AM or FM operation and by adjusting v_s relative to $\omega\phi_0$ we can get harmonic or pulse-like response. In general, we find that these devices give the best signal-to-noise ratio when $R<\omega L$ and when they are fairly strongly coupled to a tank circuit. We find that these structures form quite reliable devices, particularly when composed of the hard superconductors such as Nb and Ta, are not delicate to handle, and have a long working lifetime. A superconducting magnetometer based on these devices is in routine operation in the Laboratory of Mathematics and Physics, California Institute of Technology, Pasadena, for use in ultrasensitive magnetochemical analysis.

Acknowledgment

The authors wish to thank E. Boud and D. Lawson for their assistance in thin film and circuit fabrication.

References

[1] B. D. Josephson, "Possible new effects in superconductive tunneling," *Phys. Lett.*, vol. 1, pp. 251–253, 1962.

[2] W. C. Stewart, "Current-voltage characteristics of Josephson junctions," *Appl. Phys. Lett.*, vol. 12, pp. 277–280, 1968.
D. E. McCumber, "Effects of ac impedance on dc voltage-current characteristics of superconductor weak-link junctions," *J. Appl. Phys.*, vol. 39, pp. 3113–3118, 1968.
P. K. Hansma, G. I. Rochlin, and J. N. Sweet, "Externally shunted Josephson junctions: Generalized weak links," *Phys. Rev. B*, vol. 4, pp. 3003–3014, 1971.

[3] P. W. Anderson and A. H. Dayem, "Radio frequency effects in superconducting thin film bridges," *Phys. Rev. Lett.*, vol. 13, pp. 195–197, 1964.
P. W. Anderson, "Considerations on the flow of superfluid helium," *Rev. Mod. Phys.*, vol. 38, pp. 298–310, 1966.

[4] A. Baratoff, J. A. Blackburn, and B. Schwartz, "Current-phase relationship in short superconducting weak links," *Phys. Rev. Lett.*, vol. 25, pp. 1096–1099, Oct. 1970.
J. Bardeen and J. L. Johnson, "Josephson current flow in pure superconducting-normal-superconducting junctions," *Phys. Rev. B*, vol. 5, pp. 72–78, Jan. 1972.
T. J. Rieger, D. J. Scalapino, and J. E. Mercereau, "Time dependent superconductivity and quantum dissipation," *Phys. Rev. B*, Aug. 1972.

[5] R. K. Kirschman, H. A. Notarys, and J. E. Mercereau, "AC and DC potentials in superconducting phase-slip structures," *Phys. Lett.*, vol. 34A, pp. 209–211, 1971.

[6] P. E. Gregers-Hansen and N. T. Levinsen, "Normal state resistance as the determining parameter in the behavior of Dayem bridges with sinusoidal current-phase relations," *Phys. Rev. Lett.*, vol. 17, pp. 847–849, Sept. 1971.

[7] A. H. Silver and J. E. Zimmerman, "Quantum states and transitions in weakly connected superconducting rings," *Phys. Rev.*, vol. 157, pp. 317–341, 1967.

[8] J. E. Mercereau, "Superconducting magnetometers," *Rev. Phys. Appl.*, vol. 5, pp. 13–20, 1970.

[9] R. P. Gifford, R. A. Webb, and J. C. Wheatley, "Principles and methods of low-frequency electric and magnetic measurements using an rf-biased point-contact superconducting device," *J. Low Temp. Phys.*, vol. 6, pp. 533–610, 1972.
W. W. Webb, "Superconducting quantum magnetometers," *IEEE Trans. Magn.*, vol. MAG-8, pp. 51–60, Mar. 1972.

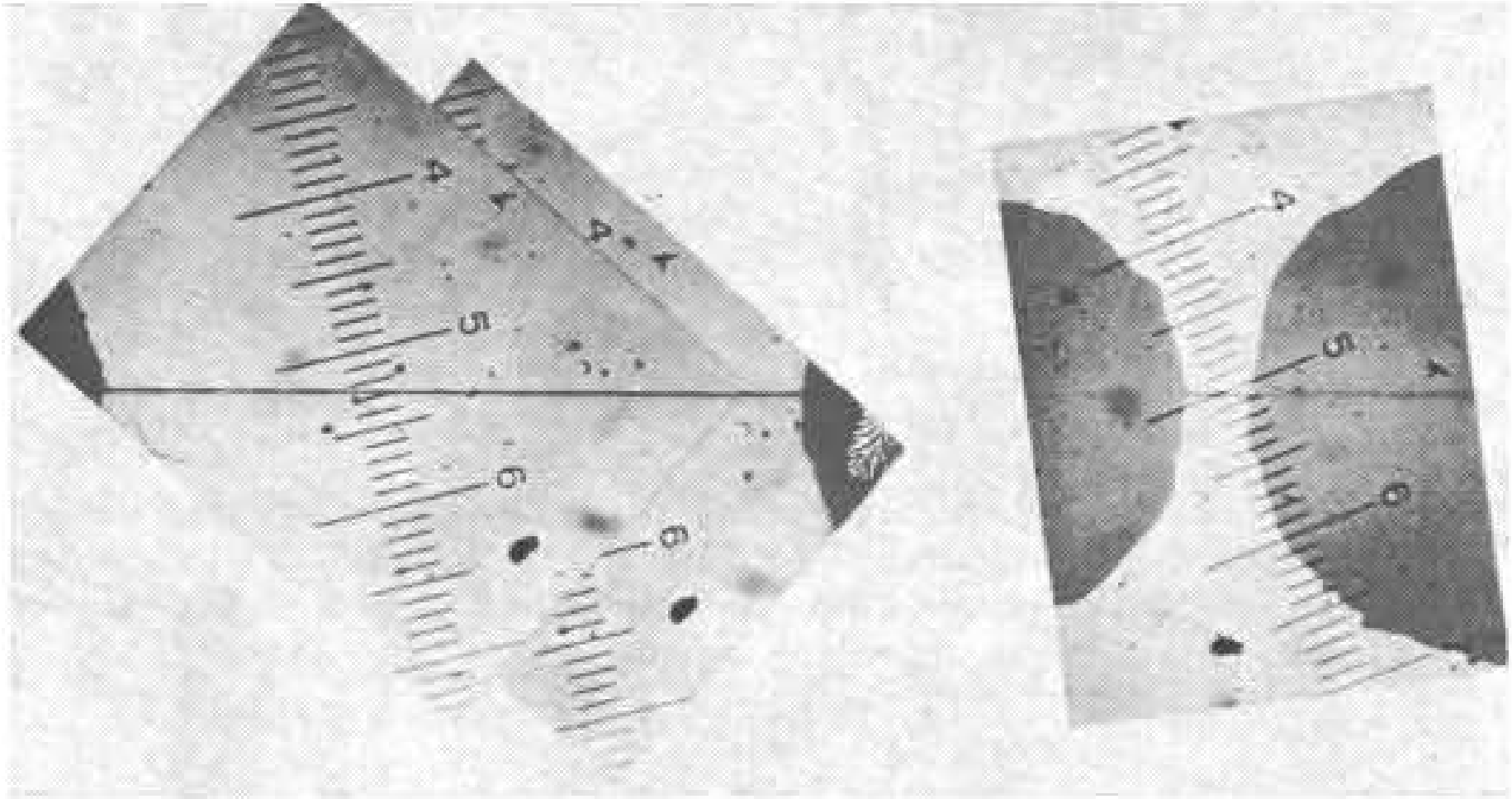

Fig. 2. Microphotograph of a phase slip junction in a hard supercon-